Experimental and Molecular Pathology 110 (2019) 104287

Contents lists available at ScienceDirect

Experimental and Molecular Pathology

journal homepage: www.elsevier.com/locate/yexmp

Long non-coding RNA TUG1 alleviates LPS-induced injury of PC-12 cells by down-regulating microRNA-127

Huajiang Zheng[1], Shanshan Hu[1], Jin Cao*, Lufeng Yao, Nan Zhang

Department of Orthopedics, Ningbo No.6 Hospital, Ningbo 315040, Zhejiang, China

ARTICLE INFO

Keywords:
Spinal cord injury
lncRNA TUG1
microRNA-127
Inflammatory injury
NF-κB/p38MAPK

ABSTRACT

The limited therapeutic strategies and the unsatisfied prognosis for spinal cord injury (SCI) make the identification of innovative therapeutic targets for SCI become very urgent. Herein, we explored the role of long non-cording RNA taurine up-regulated gene 1 (lncRNA TUG1) in lipopolysaccharide (LPS)-treated PC-12 cells and studied the downstream effector and signaling cascades. We found that LPS-induced decrease of cell viability, increase of apoptosis and release of IL-6 and TNF-α were mitigated by TUG1 overexpression. MicroRNA (miR-127) was negatively regulated by TUG1. Effects of TUG1 on LPS-treated PC-12 cells were reversed by miR-127 overexpression. Besides, TUG1 inactivated NF-κB and p38MAPK pathways in LPS-treated PC-12 cells via down-regulating miR-127. *Dynactin 4* and *protein tyrosine phosphatase* (*PTP*) were the target genes of miR-127. miR-127 regulated the NF-κB and p38MAPK pathways in PC-12 cells at least by targeting dynactin 4 and PTP. In conclusion, we discovered that TUG1 alleviated LPS-induced PC-12 cell inflammatory injury might be through down-regulating miR-127, influencing dynactin 4 and PTP, and then inactivating NF-κB and p38MAPK pathways.

1. Introduction

Spinal cord injury (SCI) is a catastrophic event caused by trauma or diseases and acting as the major cause for long-term physical impairment (O'Shea et al., 2017). It is accepted to be a global health problem that afflicts young adults and the elderly (Luk and Souter, 2017). In the United States, the National Spinal Cord Injury Statistical Center has reported that approximately 240,000–337,000 people are living with SCI, and the annual incidence is estimated to be 12,500–20,000 cases (Ma et al., 2014; Poniatowski et al., 2017). However, until now, the therapeutic strategies for SCI are very limited. It is worthy believing that searching for effective therapeutic strategies will be helpful for SCI treatment.

There are two separate processes during the progression of SCI. Initially, mechanical injuries resulting from traffic, falling, industrial or athletic accidents produce the majority of the potential deficits (Chen et al., 2018). Then, a delayed secondary damage presenting as neuronal and glial apoptosis and a neuro-inflammatory response is occurred, which causes damage and edema around the spinal cord (Babu, 2018; Rust and Kaiser, 2017). It is imperative to develop therapeutic strategies aiming to repress or alleviate the secondary damage to the spinal cord since the mechanical injuries occur suddenly and unexpectedly.

Long non-coding RNAs (lncRNAs), a heterogeneous group of RNA transcripts between 200 nucleotides and 100 kb in length, can either activate or suppress gene expression and thereby participate in diverse biological processes (Gomes et al., 2017; Yao et al., 2018). Currently, an increasing number of lncRNAs has been identified to be involved in the SCI progression. For example, lncRNA X-inactive specific transcript (XIST) is reported as a promising molecular target for SCI therapy as it induces neuronal apoptosis through blocking the phosphatase and tensin homologue/phosphatidylinositol-3 kinase/protein kinase 3 (PTEN/PI3K/AKT) pathways in rat (Gu et al., 2017). The inflammatory response of microglia after SCI is attenuated by lncRNA metastasis-associated lung adenocarcinoma transcript 1 (MALAT1) knockdown (Zhou et al., 2018). lncRNA taurine up-regulated gene 1 (TUG1) is a 7.1 kb lncRNA that was firstly identified as up-regulated genes after taurine treatment in developing mouse retinal cells (Young et al., 2005). In the last few years, more and more studies revealed that TUG1 acted as either an oncogene or a tumor suppressor in different cancers (Li et al., 2016b). TUG1 is also reported as a major regulator of cell cycle in response to DNA damage (Khalil et al., 2009). In addition, TUG1 exerts an inhibitory effect on apoptosis and inflammation in cold-injured mouse livers (Su et al., 2016). However, the role of TUG1 in SCI remains poorly studied.

* Corresponding author.
E-mail address: caojin0290@sina.com (J. Cao).
[1] Co-first authors.

https://doi.org/10.1016/j.yexmp.2019.104287
Received 27 August 2018; Received in revised form 15 July 2019; Accepted 17 July 2019
Available online 18 July 2019
0014-4800/

MicroRNAs (miRNAs/miRs) are another group of non-coding RNAs with 17–22 nucleotides in length (Burgess et al., 2018; Hammond, 2015). Many lncRNAs, including TUG1, can exert function through regulating miRNAs expression (Adams et al., 2017; Cao et al., 2017). miRNA-127 (miR-127) has been found to play pro-inflammatory roles in human cells (Ying et al., 2015). Previous research proved that suppression of miR-127 could protect *in vitro* SCI cell model (PC-12 cells) from inflammatory injury via down-regulating programmed cell death 4 gene (PDCD4) (Zhang et al., 2017).

In the present study, we induced inflammatory injury of PC-12 cells using lipopolysaccharide (LPS) to mimic secondary injury of SCI *in vitro* and explored the effects of TUG1 on LPS-treated PC-12 cells. Moreover, we tried to analyze the internal regulatory mechanism related to miR-127, as well as possible signaling pathways. We aimed to figure out innovative therapeutic targets for SCI treatments.

2. Materials and methods

2.1. Cell culture and treatment

PC-12 cell line (CRL-1721™) was obtained from American Type Culture Collection (ATCC; Manassas, VA, USA). Cells were seeded into flasks at a density of 1×10^4 cells/mL in Rosewell Park Memorial Institute (RPMI)-1640 medium (Gibco, Grand Island, NY, USA) supplemented with 10% heat-inactivated horse serum (Gibco) and 5% fetal bovine serum (Gibco). Flasks were placed in a humidified incubator filled with 5% CO_2 and 95% air at 37 °C. Culture medium was renewed every 2 to 3 days. Inflammatory injury of PC-12 cells was induced by incubation with LPS (Sigma-Aldrich, St. Louis, MO, USA) in a series of concentration for 12 h (Zhang et al., 2017).

2.2. Transfection with recombined plasmids and miRNAs

Full-length TUG1 sequence was amplified using PCR and ligated into pcDNA3.1 vector (Invitrogen, Carlsbad, CA, USA), which was referred as pc-TUG1. After sequencing, 50 pmol empty pcDNA3.1 or pc-TUG1 was transfected into PC-12 cells with the help of lipofectamine 3000 reagent (Invitrogen) for 24 h following the manufacturer's instructions. Then, the stably transfected cells were selected using culture medium containing 0.5 mg/mL G418 (Sigma-Aldrich) for approximately 4 weeks. miR-127 mimic and its negative control (NC-miRNA) were designed and synthesized by GenePharma Corporation (Shanghai, China). The oligonucleotides sequences for miR-127 mimic were: 5′-CUGAAUCUCAGAGGGCUCUGAUU-3′ (mimic sense) and 5′-UCAGAGCCCUCUGAGCUUCAGUU-3′ (mimic anti-sense). The oligonucleotides sequence for NC-miRNA was: 5′-UCACAACCUCCUAGAAAGAGUAGA-3′. Then, 100 pmol either miR-127 mimic or NC-miRNA was transfected into PC-12 cells utilizing the lipofectamine 3000 reagent, and transiently transfected cells were harvested at 72 h post-transfection. Transfection efficiencies were measured using qRT-PCR.

2.3. Cell viability assay

The Cell Counting Kit-8 (CCK-8) assay (Dojindo, Kumamoto, Japan) was used to measure the viability of PC-12 cells. Briefly, transfected or non-transfected PC-12 cells were seeded in 96-well plates with 5×10^3 cells/well and incubated at 37 °C overnight for attachment. After different treatment, 10 μL of CCK-8 solution was added into each well of the plate and the plate was placed in humidified incubator at 37 °C for 1 h. Subsequently, the absorbance of each well at 450 nm was testified using Microplate Reader (Bio-Rad, Hercules, CA, USA). Cell viability (%) was expressed as the percentage of control.

2.4. Apoptosis assay

The Annexin V-FITC Apoptosis Detection Kit (Solarbio, Beijing Solarbio Science & Technology Co., Ltd., Beijing, China) was used for detection the apoptosis of PC-12 cells. Briefly, transfected or non-transfected PC-12 cells were seeded in 6-well plates with 1×10^5 cells/well and incubated at 37 °C overnight for attachment. After different treatment, cells in each group were collected and washed with cold phosphate buffered saline (PBS) for twice. Then, cells were suspended in Binding Buffer at a density of 1×10^6 cells/mL. Subsequently, 5 μL Annexin V-FITC and 5 μL propidium iodide (PI) were added into 100 μL Binding buffer containing cells at room temperature in the dark for 25 min. After addition of 500 μL PBS, stained cells were testified by using a FACS can (Beckman Coulter, Fullerton, CA, USA). Percentage of apoptotic cells was analyzed by using the FlowJo software (Tree Star, San Carlos, CA, USA).

2.5. Reverse transcription-quantitative PCR (RT-qPCR)

After different treatment or transfection, total RNAs in PC-12 cells were extracted by using an RNeasy Mini Kit (Qiagen, Valencia, CA, USA) following the manufacturer's protocol. The expression level of TUG1 was quantified using the One Step SYBR® PrimeScript™ PLUS RT-RNA PCR kit (TaKaRa Biotechnology, Dalian, China) according to the manufacturer's instructions. For analysis the expression levels of interleukin 6 (IL-6) and tumor necrosis factor α (TNF-α), total RNA was reverse transcribed to double-stranded cDNA using the PrimeScript™ RT reagent Kit (TaKaRa) and the following real-time PCR was performed using the TB Green™ Fast qPCR Mix (TaKaRa), as suggested by the respective manufacturer's instructions. GAPDH was acted as the internal control of TUG1, IL-6 and TNF-α. For analysis the expression level of miR-127, a two-step real-time RT-PCR for miRNAs directly from cultured cell lysates was performed using the TaqMan® MicroRNA Cells-to-CT™ Kit (Invitrogen) according to the supplier's protocol, and U6 was acted as the internal control. Data were quantified using $2^{-\Delta\Delta Ct}$ method (Livak and Schmittgen, 2001) and presented as the ratios of control. Each sample was analyzed in triplicate, and all experiments were carried out three times independently.

2.6. Dual luciferase reporter assay

The 3′-untranslated regions (3′UTR) fragments of *dynactin 4* (*p62*) and *Protein tyrosine phosphatase* (*PTP*) containing the predicated miR-127 binding sites were amplified by PCR and cloned into pmirGlO Dual-luciferase miRNA Target Expression Vector (Promega, Madison, WI, USA) to form the reporter vector Dynactin 4-wild-type (Dynactin 4-wt) and PTP-wild-type (PTP-wt). To mutate the predicated binding sites of miR-127 in 3′UTR of *dynactin 4* and *PTP*, the sequences of putative binding sites were replaced, amplified by PCR and also cloned into pmirGlO Dual-luciferase miRNA Target Expression Vector to form the reporter vector Dynactin 4-mutated-type (Dynactin 4-mut) and PTP-mutated-type (PTP-mut). After that, the vectors and miR-127 mimic were co-transfected and the relative luciferase activity was tested by Dual-Luciferase Reporter Assay System (Promega, Madison, WI, USA).

2.7. Western blot analysis

After different treatment or transfection, the whole cell lysates were obtained using RIPA buffer (Beyotime, Shanghai, China) containing 1 mM PMSF (Beyotime). Protein concentration in the supernatant was quantified using the BCA™ Protein Assay Kit (Pierce, Appleton, WI, USA). Then, equal concentration of proteins was fractioned individually on SDS-PAGE gels and electro-transferred to nitrocellulose membranes, followed by blocking in 5% non-fat milk. Those nitrocellulose strips were incubated with primary antibodies against Bcl-2 (ab196495), Bax (ab53154), IL-6 (ab9324), TNF-α (ab6671), p65 (ab16502), phospho (p)-p65 (ab28856), p38 mitogen-activated protein kinase (p38MAPK, ab170099), p-p38MAPK (ab47363), β-actin (ab8227, all Abcam, Cambridge, UK), caspase-3 (#9662), inhibitor of nuclear factor kappa B

(IκBα, #4812) or p-IκBα (#2859, all Cell Signaling Technology, Beverly, MA, USA) at 4 °C overnight. Subsequently, those membranes were incubated with secondary antibody marked by horseradish peroxidase (goat anti-rabbit ab97051 or goat anti-mouse ab6789, Abcam) at room temperature for 2 h in the dark. Finally, the proteins in the membranes were visualized using an ECL Western blotting detection reagent (GE Healthcare, Braunschweig, Germany). The intensities of bands were analyzed by the ImageJ software (National Institutes of Health, Bethesda, MA, USA).

2.8. Statistical analysis

Experiments were performed in triplicate with three repeats. Results were presented as the mean ± standard deviation (SD). Data analysis was carried out using Graphpad Prism 5 software (GraphPad, San Diego, CA, USA). The *P*-values were calculated using the one-way analysis of variance (ANOVA) or Student's *t*-test. *P* values of < 0.05 were deemed statistically significant.

3. Results

3.1. LPS induced PC-12 cell inflammatory injury

The adequate dosage of LPS was explored according to the results of CCK-8 assay. As evidenced in Fig. 1A, viability of PC-12 cells was significantly reduced after 2 μg/mL LPS ($P < .05$), 5 μg/mL LPS ($P < .01$) and 10 μg/mL LPS ($P < .001$) stimulation, compared with untreated cells. No marked decrease of cell viability was observed when the dosage of LPS was 1 μg/mL LPS. Since cell viability was reduced to 52.48 ± 3.51% after stimulation with 5 μg/mL LPS, 5 μg/mL LPS stimulation was chosen for subsequent experiments. Flow cytometry assay showed that the percentage of apoptotic cells was dramatically elevated after 5 μg/mL LPS treatment relative to the untreated cells ($P < .001$, Fig. 1B). Similar results were found in Fig. 1C, which displayed that 5 μg/mL LPS treatment down-regulated the expression level of Bcl-2, while up-regulated the expression levels of Bax and cleaved caspase-3 in PC-12 cells. In addition, both mRNA and protein expression levels of inflammatory cytokines, IL-6 and TNF-α, were up-regulated in PC-12 cells after 5 μg/mL LPS stimulation, compared with the control group ($P < .01$ or $P < .001$ in mRNA level, Fig. 1D-1E). Those results indicated that LPS could induce PC-12 cell inflammatory injury.

3.2. Overexpression of TUG1 attenuated LPS-induced inflammatory injury of PC-12 cells

The expression level of TUG1 in PC-12 cells after 5 μg/mL LPS stimulation was measured using qRT-PCR. Fig. 2A showed that 5 μg/mL LPS stimulation significantly reduced the expression level of TUG1 in PC-12 cells ($P < .01$). pc-TUG1 was transfected into PC-12 cells to up-regulate the expression level of TUG1. Fig. 2B displayed that the expression level of TUG1 in PC-12 cells transfected with pc-TUG1 was prominently higher than that in PC-12 cells transfected with pcDNA3.1 ($P < .01$), suggesting that TUG1 was overexpressed successfully after transfection. Then, effects of TUG1 overexpression on PC-12 cell viability loss, apoptosis and release of inflammatory cytokines after 5 μg/mL LPS treatment were studied. We found that TUG1 overexpression effectively attenuated the LPS-induced PC-12 cell injury, showing significant increase of cell viability ($P < .05$, Fig. 2C), obvious reduction of apoptotic cells ($P < .05$, Fig. 2D), observable down-regulation of Bax and cleaved caspase-3 as well as up-regulation of Bcl-2 (Fig. 2E), and marked decreases of the mRNA and protein expression levels of IL-6 and TNF-α ($P < .05$ or $P < .01$ in mRNA level, Fig. 2F–G). Those results collectively indicated that TUG1 overexpression could protect PC-12 cells from LPS-induced inflammatory injury.

3.3. Overexpression of TUG1 down-regulated miR-127 expression in PC-12 cells

The expression level of miR-127 in PC-12 cells after 5 μg/mL LPS stimulation was also measured. The result in Fig. 3A presented that 5 μg/mL LPS stimulation remarkably up-regulated the expression level of miR-127 in PC-12 cells ($P < .01$). The interaction between miR-127 and TUG1 was studied to reveal the regulatory mechanism of TUG1. As evidenced in Fig. 3B, miR-127 expression level in PC-12 cells over-expressing TUG1 was markedly lower than the in pcDNA3.1-transfected cells ($P < .01$). Bioinformatics analysis found that TUG1 could bind to the sequence of miR-127. The potential binding site was shown in Fig. 3C. These findings suggested that TUG1 negatively regulated the miR-127 expression in PC-12 cell might be targeting miR-127 sequence and hinted that TUG1-induced down-regulation of miR-127 might participate in the effects of TUG1 on LPS-treated PC-12 cells.

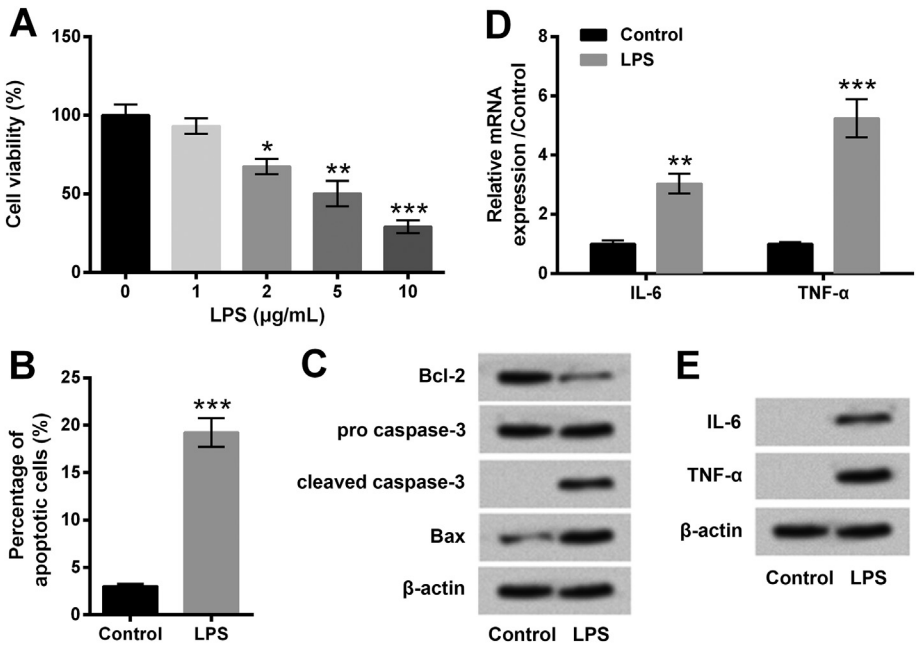

Fig. 1. LPS induced PC-12 cell inflammatory injury. (A) PC-12 cells were stimulated with increasing dosages of LPS (1, 2, 5 and 10 μg/mL) for 12 h, and untreated cells were acted as control. Cell viability was detected by CCK-8 assay. PC-12 cells were stimulated with 5 μg/mL LPS for 12 h, and untreated cells were acted as control. (B) Percentage of apoptotic cells was assessed by flow cytometry assay. (C) Protein expression levels of Bcl-2, Casapse 3 and Bax were evaluated using western blot analysis. (D) The mRNA expression levels of IL-6 and TNF-α were measured by RT-qPCR. (E) The protein expression levels of IL-6 and TNF-α were evaluated by Western blot analysis. Data were presented as the mean ± standard deviation (SD) of three independent experiments. For western blotting, the most representative images were shown. *, $P < .05$; **, $P < .01$; ***, $P < .001$.

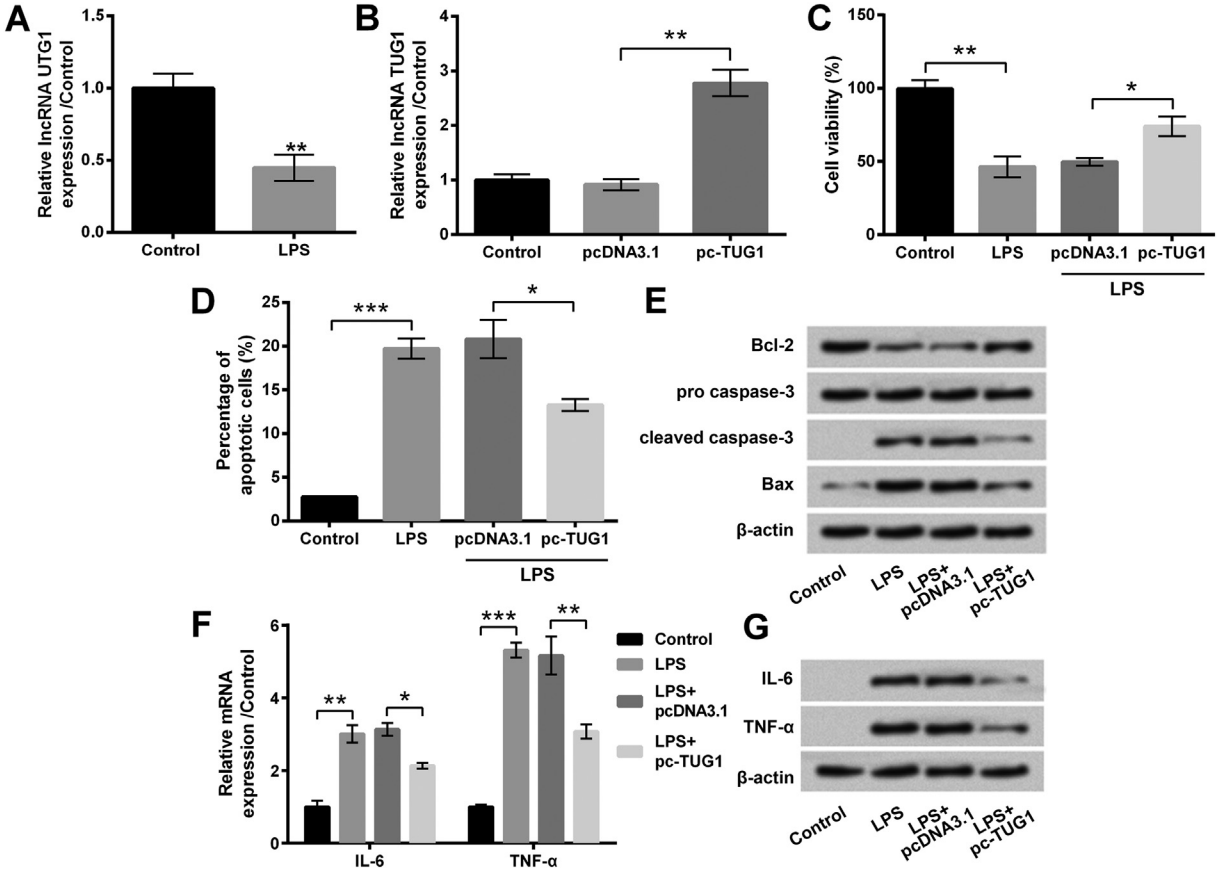

Fig. 2. Overexpression of TUG1 attenuated LPS-induced inflammatory injury of PC-12 cells. (A) PC-12 cells were stimulated with 5 μg/mL LPS for 12 h, the expression level of TUG1 was measured using qRT-PCR. (B) PC-12 cells were transfected with pcDNA3.1 or pc-TUG1, and non-transfected cells were acted as control. The expression level of TUG1 was measured by RT-qPCR. pcDNA3.1 or pc-TUG1 transfected PC-12 cells or non-transfected cells were stimulated with 5 μg/mL LPS for 12 h. Untreated cells were acted as control. (C) Cell viability was detected by CCK-8 assay. (D) Percentage of apoptotic cells was assessed by flow cytometry assay. (E) Protein expressions level of Bcl-2, Casapse 3 and Bax were evaluated by western blot analysis. (F) The mRNA expression levels of IL-6 and TNF-α were measured by RT-qPCR. (G) The protein expression levels of IL-6 and TNF-α were evaluated by Western blot analysis. Data were presented as the mean ± standard deviation (SD) of three independent experiments. For western blotting, the most representative images were shown. *, $P < .05$; **, $P < .01$; ***, $P < .001$.

3.4. TUG1 alleviated LPS-induced PC-12 cell inflammatory injury by down-regulating miR-127

Due to the negative correlation between miR-127 and TUG1, we next studied whether down-regulation of miR-127 was the reason for the protective effect of TUG1 on LPS-treated PC-12 cells. After miR-127 mimic transfection, we found that the expression level of miR-127 in PC-12 cells was notably increased ($P < .01$, Fig. 4A). Then, PC-12 cells were co-transfected with pc-TUG1 (pcDNA3.1) and miR-127 mimic (NC-miRNA), followed by incubation with LPS. Results showed that the effects of TUG1 overexpression on LPS-treated PC-12 cells were effectively reversed by miR-127 overexpression, as evidenced by miR-127 overexpression significantly reduced cell viability ($P < .05$, Fig. 4B), elevated the rate of apoptotic cells ($P < .01$, Fig. 4C), up-regulated the expression levels of Bax and cleaved caspase-3 as well as down-regulated the expression level of Bcl-2 (Fig. 4D), and up-regulated the mRNA and protein expression of IL-6 and TNF-α ($P < .05$ or $P < .01$ in mRNA level, Fig. 4E–F), compared with the LPS + pc-TUG1 + NC-

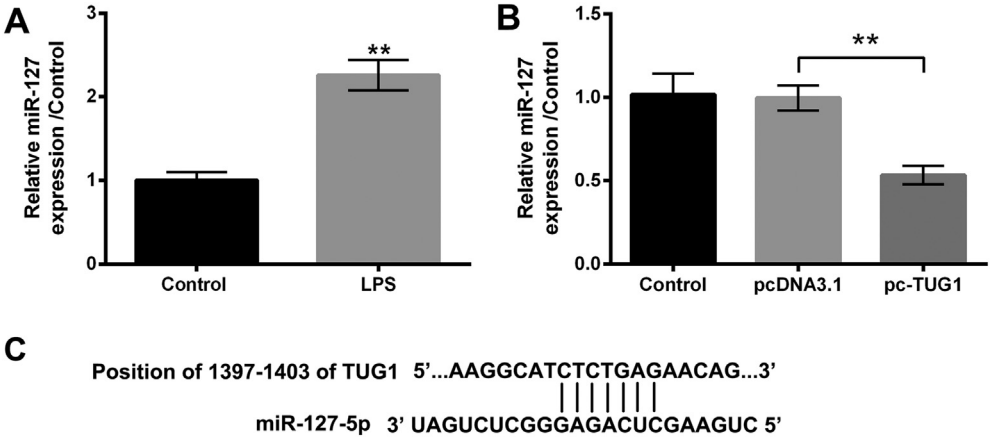

Fig. 3. TUG1 down-regulated miR-127 expression in PC-12 cells. (A) PC-12 cells were stimulated with 5 μg/mL LPS for 12 h, the expression level of miR-127 was measured using qRT-PCR. (B) PC-12 cells were transfected with pcDNA3.1 or pc-TUG1, and non-transfected cells were acted as control. The expression level of miR-127 was determined by RT-qPCR. (C) The potential binding site between TUG1 and miR-127-5p. Data were presented as the mean ± standard deviation (SD) of three independent experiments. **, $P < .01$.

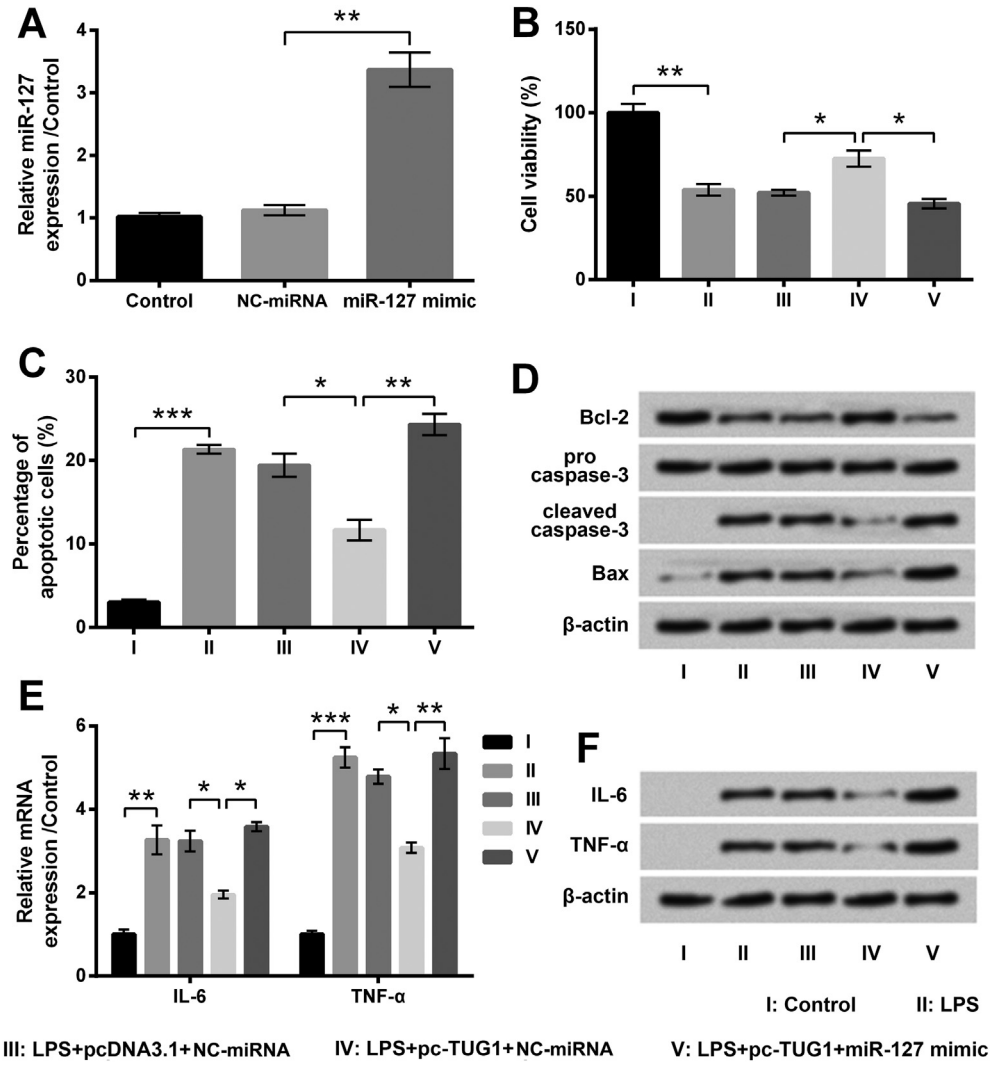

Fig. 4. TUG1 alleviated LPS-induced PC-12 cell inflammatory injury through down-regulated miR-127. (A) PC-12 cells were transfected with miR-127 mimic or its negative control (NC-miRNA), and non-transfected cells were acted as control. The expression level of miR-127 was measured by RT-qPCR. PC-12 cells were co-transfected with pc-TUG1 (pcDNA3.1) and miR-127 mimic (NC-miRNA), as well as stimulated with 5 μg/mL LPS for 12 h. Untreated cells were acted as control. (B) Cell viability was detected by CCK-8 assay. (C) Percentage of apoptotic cells was assessed by flow cytometry assay. (D) Protein expression levels of Bcl-2, Caspase 3 and Bax were evaluated by western blot analysis. (E) mRNA expression levels of IL-6 and TNF-α were measured by RT-qPCR. (F) Protein expression levels of IL-6 and TNF-α were evaluated by Western blot analysis. Data were presented as the mean ± standard deviation (SD) of three independent experiments. For western blotting, the most representative images were shown. *, $P < .05$; **, $P < .01$; ***, $P < .001$.

miRNA group. These results collectively indicated that TUG1 protected PC-12 cells against LPS-induced inflammatory injury at least in part through down-regulating miR-127.

3.5. TUG1 inactivated NF-κB and p38MAPK pathways in LPS-treated PC-12 cells via down-regulation of miR-127

The activation of NF-κB and p38MAPK pathways in PC-12 cells was studied after pc-TUG1 and/or miR-127 mimic transfection followed by LPS treatment. Fig. 5A and B displayed that miR-127 overexpression notably activated NF-κB and p38MAPK pathways in PC-12 cells via increasing the expression rates of p/t-IκBα, p/t-p65 and p/t-p38MAPK ($P < .05$). Moreover, Fig. 5C and D showed that the expression rates of p/t-IκBα, p/t-p65 and p/t-p38MAPK were all significantly increased by LPS treatment (both $P < .01$), and those increases were observably abrogated by TUG1 overexpression ($P < .05$ or $P < .01$). In addition, the effects of TUG1 overexpression on the expression rates of p/t-IκBα, p/t-p65 and p/t-p38MAPK were all markedly reversed by miR-127 overexpression (both $P < .01$). These above results indicated that TUG1 could inactivate NF-κB and p38MAPK pathways in LPS-treated PC-12 cells via down-regulation of miR-127.

3.6. Dynactin 4 and PTP were the target genes of miR-127 in PC-12 cells

Bioinformatics analysis using TargetScanHuman 7.1 (http://www.targetscan.org/vert-71) found that both *dynactin 4* and *PTP* were the target genes of miR-127. The potential binding sites were displayed in Fig. 6A and B. Moreover, the results of dual-luciferase reporter assay showed that co-transfection with miR-127 mimic and Dynactin 4-wt (or PTP-wt) significantly reduced the relative luciferase activity ($P < .05$, Fig. 6C and D). These results suggested that Dynactin 4 and PTP were the target genes of miR-127 in PC-12 cells and implied that miR-127 regulated the NF-κB and p38MAPK pathways in PC-12 cells at least by targeting dynactin 4 and PTP.

4. Discussion

Considering the limited therapeutic strategies and the unsatisfied prognosis for SCI, we explored the role of TUG1 in LPS-induced PC-12 cell inflammatory injury in order to find innovative therapeutic targets for SCI. Herein, we reported for the first time that TUG1 could attenuate LPS-induced inflammatory injury of PC-12 cells and down-regulate miR-127 expression. In the meantime, we found that miR-127 overexpression could reverse the effects of TUG1 on LPS-treated PC-12 cells. Besides, the NF-κB and p38MAPK pathways in PC-12 cells might be repressed by TUG1 via regulation of miR-127 targeting Dynactin 4 and PTP.

PC-12 cells have an embryonic origin from the neural crest and contain a mixture of neuroblastic cells and eosinophilic cells (Guan et al., 2017). This cell line is a widely used cell model for studying SCI (Rong et al., 2018). SCI is characterized by an aggressive inflammation and neuronal degeneration (Didangelos et al., 2016). LPS, an endotoxin

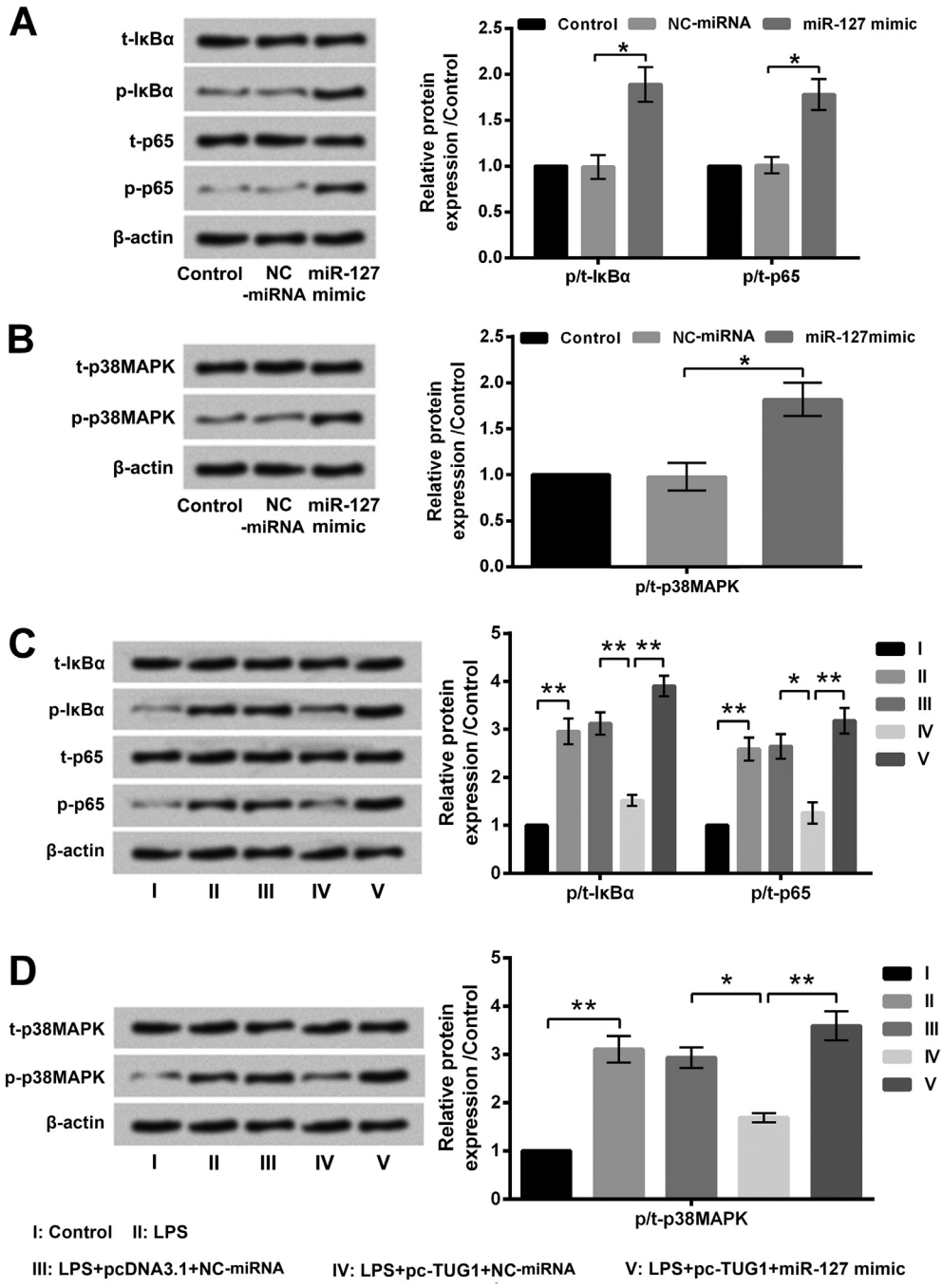

Fig. 5. TUG1 inactivated NF-κB and p38MAPK pathways in LPS-treated PC-12 cells through down-regulated miR-127. PC-12 cells were transfected with miR-127 mimic or its negative control (NC), the protein expression levels of key kinases in the NF-κB pathway (A) and p38MAPK pathway (B) were evaluated by Western blot analysis. PC-12 cells were co-transfected with pc-TUG1 (pcDNA3.1) and miR-127 mimic (NC-miRNA), as well as stimulated with 5 μg/mL LPS for 12 h. Untreated cells were acted as control. Protein expression levels of key kinases in the NF-κB pathway (C) and p38MAPK pathway (D) were evaluated by Western blot analysis. Data were presented as the mean ± SD of three independent experiments. The most representative images were shown. *, $P < .05$; **, $P < .01$.

in the outer membranes of gram-negative bacteria, can activate NF-κB pathway in cells, leading to release of large amount of inflammatory cytokines, such as TNF-α and IL-6 (Noble et al., 2018). Therefore, in our study, we constructed inflammatory injury model of PC-12 cells using LPS to mimic second injury of SCI, and cell viability, apoptosis and release of inflammatory cytokines (TNF-α and IL-6) were measured to evaluate cell injury. Apoptosis and inflammatory response are two prominent features for secondary injury of SCI (Cong and Chen, 2016). The mitochondrial-pathway controlled by the Bcl-2 protein family and the following caspase-dependent pathway are responsible for apoptosis after SCI (Liu et al., 1997). Down-regulation of Bcl-2 and up-regulation of Bax and cleaved caspase-3 after LPS treatments supported the elevated apoptotic cells analyzed by flow cytometry. In our study, the reduced cell viability, enhanced apoptosis and release of TNF-α and IL-6 illustrated that inflammatory injury of PC-12 cells was induced successfully by LPS treatment.

The expression level of TUG1 was reduced after LPS treatment. After transfection, the expression level of TUG1 was stably overexpressed in PC-12 cells and the effects of TUG1 overexpression on LPS-induced inflammatory injury in PC-12 cells were assessed. Results in our study showed that TUG1 overexpression could effectively attenuate inflammatory injury of PC-12 cells. Effects of TUG1 on apoptosis are dependent on the specific cell type. Yin et al. have demonstrated that TUG1 silence promotes apoptosis of pancreatic β cells both in vitro and in vivo (Yin et al., 2015). Zhang et al. reported that in LPS-treated H9c2 cells, apoptosis was reduced by TUG1 overexpression (Zhang et al., 2018). Su et al. also reported that apoptosis of mouse liver cells induced by cold was repressed by TUG1 (Su et al., 2016). However, TUG1 shows a pro-apoptotic role in glioma cancer cells (Li et al., 2016a). One possible reason for the opposite effects of TUG1 on cell apoptosis might be

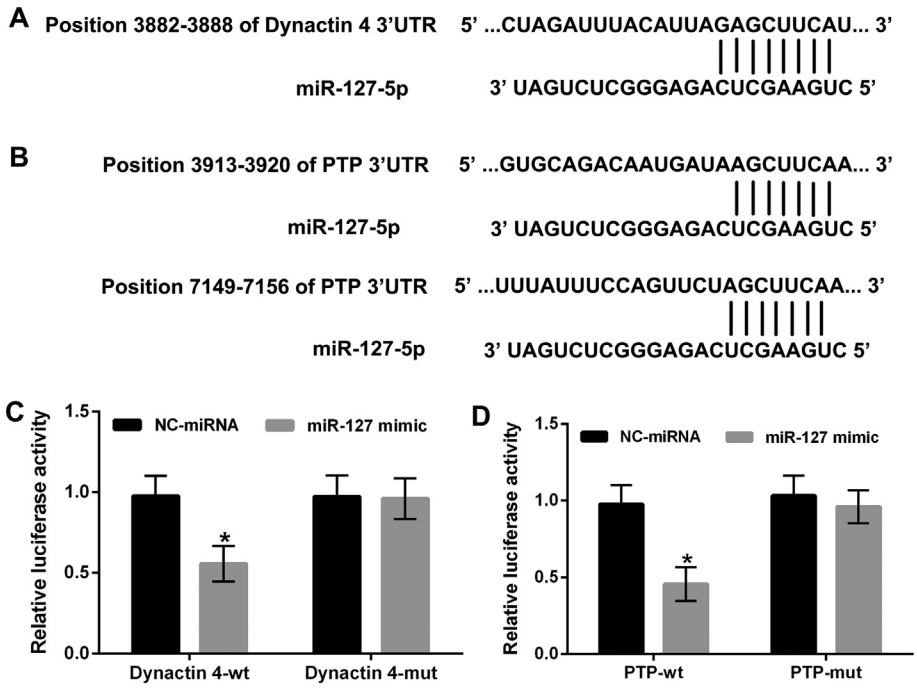

Fig. 6. Dynactin 4 and PTP were the target genes of miR-127 in PC-12 cells. (A) The potential binding site between the 3′-untranslated regions (3′UTR) of *Dynactin 4* and miR-127-5p. (B) The potential binding sites between the 3′UTR of *PTP* and miR-127-5p. (C and D) The relative luciferase activity was tested by dual luciferase reporter assay after co-transfection with miR-127 mimic (or NC-miRNA) and Dynactin 4-wt (or PTP-wt). Data were presented as the mean ± SD of three independent experiments. *, $P < .05$.

the diversity of downstream factors in different cell types. In this research, the anti-inflammatory effects of TUG1 in PC-12 cells were consistent with that in mouse liver cells (Su et al., 2016) and murine chondrogenic ATDC5 cells (Liang and Ren, 2018).

For the research on regulatory mechanism, we focused on the downstream miRNAs of TUG1. TUG1 can bound to the polycomb repressive complex 2 (PRC2) and elicit its biological activity through epigenetic silence of downstream effector (Zhang et al., 2014). miR-127 is embedded in a CpG island region and it can be epigenetically silenced by both promoter hypermethylation and histone modifications (Saito et al., 2006). Therefore, we further studied the relationship between TUG1 and miR-127. Results in our study showed that there was a negative correlation between TUG1 and miR-127, and a possible rational explanation was the epigenetic regulation related to PRC2. Moreover, bioinformatics analysis found that TUG1 could bind to the sequence of miR-127. Besides, we also found that miR-127 overexpression could abrogate the effects of TUG1 on LPS-treated PC-12 cells, which verified that down-regulation of miR-127 was a reason for the protective effects of TUG1 in LPS-treated PC-12 cells. The effects of miR-127 overexpression on inflammatory injury of PC-12 cells were consistent with a previous study by Zhang et al., in which miR-127 silence protected PC-12 cells against inflammatory injury induced by LPS (Zhang et al., 2017).

The NF-κB and p38MAPK pathways are both closely associated with inflammation and apoptosis, which have been found to be abnormally activated in cells following SCI (Crown et al., 2008; Han et al., 2012). Previous study reported that the NF-κB pathway was inhibited by TUG1 overexpression in LPS-treated H9c2 cells (Zhang et al., 2018). In our study, we found that these two signaling pathways in LPS-treated PC-12 cells were both significantly inhibited by TUG1 overexpression. Overexpression of miR-127 activated NF-κB and p38MAPK pathways in PC-12 cells and reversed the effects of TUG1 on LPS-treated PC-12 cells. The effects of miR-127 on activation of the NF-κB and p38MAPK pathways were consistent with the study by Shi et al. (Shi et al., 2017) and the study by Li et al. (Li et al., 2017). Dynactin 4 is an up-stream factor of NF-κB pathway (Shrum et al., 2009). PTP is an up-stream factor of p38MAPK pathway (Gum et al., 2003). Bioinformatics analysis using TargetScamHuman 7.1 (http://www.targetscan.org/vert_71/) found that both *dynactin 4* and *PTP* were the target mRNAs of miR-127 in cells. Moreover, co-transfection with miR-127 mimic and Dynactin 4-wt (or PTP-wt) significantly reduced the relative luciferase activity. These results suggested that miR-127 regulated the NF-κB and p38MAPK pathways in PC-12 cells at least via targeting dynactin 4 and PTP.

In conclusion, this study discovered that TUG1 attenuated LPS-induced PC-12 cell inflammatory injury possibly through down-regulation of miR-127 and then inactivation of NF-κB and p38MAPK pathways. The effective protective influence of TUG1 on LPS-treated PC-12 cells indicated the therapeutic potential of TUG1 for SCI, and miR-127 might also be a therapeutic target for SCI therapy. More experiments performed in animals are needed in the future to support the conclusion in this study.

Acknowledgements

This research did not receive any specific grant from funding agencies in the public, commercial, or not-for-profit sectors.

Conflict of interest statement

The authors declare that they have no conflicts of interest with the contents of this article.

References

Adams, B.D., et al., 2017. Targeting noncoding RNAs in disease. J. Clin. Invest. 127, 761–771.
Babu, J., 2018. Spinal cord injury. In: Eltorai, A.E.M. (Ed.), Essential Orthopedic Review: Questions and Answers for Senior Medical Students. Springer International Publishing, Cham, pp. 227–229.
Burgess, K.S., et al., 2018. Variants in the CYP2B6 3'UTR Alter in vitro and in vivo CYP2B6 activity: potential role of MicroRNAs. Clin. Pharmacol. Ther. 104, 130–138.
Cao, J., et al., 2017. TUG1 promotes osteosarcoma tumorigenesis by upregulating EZH2 expression via miR-144-3p. Int. J. Oncol. 51, 1115–1123.
Chen, D., et al., 2018. Administration of chlorogenic acid alleviates spinal cord injury via TLR4/NFkappaB and p38 signaling pathway antiinflammatory activity. Mol. Med. Rep. 17, 1340–1346.
Cong, L., Chen, W., 2016. Neuroprotective effect of Ginsenoside Rd in spinal cord injury rats. Basic Clin Pharmacol Toxicol. 119, 193–201.
Crown, E.D., et al., 2008. Activation of p38 MAP kinase is involved in central neuropathic pain following spinal cord injury. Exp. Neurol. 213, 257–267.
Didangelos, A., et al., 2016. High-throughput proteomics reveal alarmins as amplifiers of

tissue pathology and inflammation after spinal cord injury. Sci. Rep. 6, 21607.
Gomes, C.P.C., et al., 2017. The function and therapeutic potential of long non-coding RNAs in cardiovascular development and disease. Molecular Therapy. Nucleic Acids. 8, 494–507.
Gu, S., et al., 2017. Long coding RNA XIST contributes to neuronal apoptosis through the downregulation of AKT phosphorylation and is negatively regulated by miR-494 in rat spinal cord injury. Int. J. Mol. Sci. 18.
Guan, J., et al., 2017. Triptolide induces DNA breaks, activates caspase-3-dependent apoptosis and sensitizes B-cell lymphoma to poly(ADP-ribose) polymerase 1 and phosphoinositide 3-kinase inhibitors. Oncol. Lett. 14, 4965–4970.
Gum, R.J., et al., 2003. Antisense protein tyrosine phosphatase 1B reverses activation of p38 mitogen-activated protein kinase in liver of ob/ob mice. Mol. Endocrinol. 17, 1131–1143.
Hammond, S.M., 2015. An overview of microRNAs. Adv. Drug Deliv. Rev. 87, 3–14.
Han, X., et al., 2012. Targeting IKK/NF-kappaB pathway reduces infiltration of inflammatory cells and apoptosis after spinal cord injury in rats. Neurosci. Lett. 511, 28–32.
Khalil, A.M., et al., 2009. Many human large intergenic noncoding RNAs associate with chromatin-modifying complexes and affect gene expression. Proc. Natl. Acad. Sci. U. S. A. 106, 11667–11672.
Li, J., et al., 2016a. LncRNA TUG1 acts as a tumor suppressor in human glioma by promoting cell apoptosis. Exp Biol Med (Maywood). 241, 644–649.
Li, P., et al., 2016b. MicroRNAs in laryngeal cancer: implications for diagnosis, prognosis and therapy. Am. J. Transl. Res. 8, 1935–1944.
Li, Q., et al., 2017. miR-127 contributes to ventilator-induced lung injury. Mol. Med. Rep. 16, 4119–4126.
Liang, Z., Ren, C., 2018. Emodin attenuates apoptosis and inflammation induced by LPS through up-regulating lncRNA TUG1 in murine chondrogenic ATDC5 cells. Biomed. Pharmacother. 103, 897–902.
Liu, X.Z., et al., 1997. Neuronal and glial apoptosis after traumatic spinal cord injury. J. Neurosci. 17, 5395–5406.
Livak, K.J., Schmittgen, T.D., 2001. Analysis of relative gene expression data using real-time quantitative PCR and the 2(− Delta Delta C(T)) method. Methods. 25, 402–408.
Luk, K.H.K., Souter, M.J., 2017. Spinal cord injury. In: Khan, Z.H. (Ed.), Challenging Topics in Neuroanesthesia and Neurocritical Care. Springer International Publishing, Cham, pp. 83–95.
Ma, V.Y., et al., 2014. Incidence, prevalence, costs, and impact on disability of common conditions requiring rehabilitation in the United States: stroke, spinal cord injury, traumatic brain injury, multiple sclerosis, osteoarthritis, rheumatoid arthritis, limb loss, and back pain. Arch. Phys. Med. Rehabil. 95, 986–995.e1.
Noble, B.T., et al., 2018. The spleen as a neuroimmune interface after spinal cord injury. J. Neuroimmunol. 321, 1–11.
O'Shea, T.M., et al., 2017. Cell biology of spinal cord injury and repair. J. Clin. Invest. 127, 3259–3270.
Poniatowski, L.A., et al., 2017. Analysis of the role of CX3CL1 (Fractalkine) and its receptor CX3CR1 in traumatic brain and spinal cord injury: insight into recent advances in actions of neurochemokine agents. Mol. Neurobiol. 54, 2167–2188.
Rong, F., et al., 2018. Methotrexate remediates spinal cord injury in vivo and in vitro via suppression of endoplasmic reticulum stress-induced apoptosis. Exp Ther Med. 15, 4191–4198.
Rust, R., Kaiser, J., 2017. Insights into the dual role of inflammation after spinal cord injury. J. Neurosci. 37, 4658–4660.
Saito, Y., et al., 2006. Specific activation of microRNA-127 with downregulation of the proto-oncogene BCL6 by chromatin-modifying drugs in human cancer cells. Cancer Cell 9, 435–443.
Shi, L., et al., 2017. miR-127 promotes EMT and stem-like traits in lung cancer through a feed-forward regulatory loop. Oncogene. 36, 1631–1643.
Shrum, C.K., et al., 2009. Stimulated nuclear translocation of NF-kappaB and shuttling differentially depend on dynein and the dynactin complex. Proc. Natl. Acad. Sci. U. S. A. 106, 2647–2652.
Su, S., et al., 2016. Overexpression of the long noncoding RNA TUG1 protects against cold-induced injury of mouse livers by inhibiting apoptosis and inflammation. FEBS J. 283, 1261–1274.
Yao, Z., et al., 2018. Long non-coding RNA NRON is downregulated in HCC and suppresses tumour cell proliferation and metastasis. Biomed. Pharmacother. 104, 102–109.
Yin, D.D., et al., 2015. Downregulation of lncRNA TUG1 affects apoptosis and insulin secretion in mouse pancreatic beta cells. Cell. Physiol. Biochem. 35, 1892–1904.
Ying, H., et al., 2015. MiR-127 modulates macrophage polarization and promotes lung inflammation and injury by activating the JNK pathway. J. Immunol. 194, 1239–1251.
Young, T.L., et al., 2005. The noncoding RNA taurine upregulated gene 1 is required for differentiation of the murine retina. Curr. Biol. 15, 501–512.
Zhang, E., et al., 2014. P53-regulated long non-coding RNA TUG1 affects cell proliferation in human non-small cell lung cancer, partly through epigenetically regulating HOXB7 expression. Cell Death Dis. 5, e1243.
Zhang, Z., et al., 2017. Suppression of miR-127 protects PC-12 cells from LPS-induced inflammatory injury by downregulation of PDCD4. Biomed. Pharmacother. 96, 1154–1162.
Zhang, H., et al., 2018. Long non-coding RNA TUG1 inhibits apoptosis and inflammatory response in LPS-treated H9c2 cells by down-regulation of miR-29b. Biomed. Pharmacother. 101, 663–669.
Zhou, H.J., et al., 2018. Long noncoding RNA MALAT1 contributes to inflammatory response of microglia following spinal cord injury via the modulation of a miR-199b/IKKbeta/NF-kappaB signaling pathway. Am J Physiol Cell Physiol. 315, C52–c61.